

## REFRACTION OF LASER BEAM PROPAGATING ALONG SURFACE HORIZONTAL PATH

V.A. Banakh and I.N. Smalikho

*Institute of Atmospheric Optics,  
Siberian Branch of the Russian Academy of Sciences, Tomsk  
Received March 12, 1998*

*In this paper we analyze the influence of thermal stability of the atmosphere on the refraction of laser beams propagating along surface horizontal paths. It is shown that under unstable atmospheric conditions a laser beam can hit to the same point at the receiving plane along two trajectories. It gives two different refraction angles due to focusing atmospheric lens, which is caused by unstable stratification of temperature. The difference between these trajectories decreases with increasing the turbulent flux of heat. Beginning with the definite critical value of heat flux, a laser beam on horizontal path does not hit to the given point. The estimates of maximal length of path between two points where steady optical connection can occur at unstable atmospheric stratification are presented in the paper.*

### 1. INTRODUCTION

Phenomenon of light refraction in the atmosphere was studied theoretically and experimentally during many years, and many of the fundamental and remarkable results in this field were generalized in a series of published monographs (see, for example, Refs. 1-4). Of special interest are Refs. 1 and 5, where the Monin-Obukhov similarity theory was first used for evaluating the optical refraction along the surface paths and some optical phenomena observed in the atmosphere are explained.

At the same time, refraction of laser beams propagating in the surface layer was not yet directly analyzed, and peculiarities of this phenomenon for narrow light beams depending on thermal stability of the atmosphere were not studied.

### 2. FORMULATION OF THE PROBLEM

In laser beam propagating in the atmosphere, the beam lateral wander occurs due to refraction on inhomogeneities of the air refractive index. The equation for the vector of centroid of the laser beam intensity distribution  $\rho_c(x) = \{z_c, y_c\}$  in the observation plane  $\rho = \{z', y'\}$  at a distance  $x$  from the source, characterizing the beam drift from the initial direction of propagation, is of the following form<sup>6</sup>:

$$\frac{d^2 \rho_c(x)}{dx^2} = \frac{\int_{-\infty}^{+\infty} \int_{-\infty}^{+\infty} d^2 \rho I(x, \rho) \nabla_{\rho} n(x, \rho)}{\int_{-\infty}^{+\infty} \int_{-\infty}^{+\infty} d^2 \rho I(x, \rho)}, \tag{1}$$

where  $I(x, \rho)$  is the intensity distribution of a laser beam,  $\nabla_{\rho} = \{d/dz, d/dy\}$ ,  $n$  is the air refractive index. The boundary condition in Eq. (1) is given by the expression  $\rho_c(0) = \{0, 0\}$  and  $d\rho_c(0)/dx = \{\alpha, 0\}$ , where  $\alpha$  is the angle (in radians) at which the laser beam is directed relative to the  $x$  axis.

The regular change of the refractive index along the vertical coordinate  $z'$  makes a basic contribution to the beam wander. Therefore, we neglect the turbulent fluctuations of the refractive index and the horizontal beam displacement in Eq. (1). Further we assume that the typical scales of variation of the vertical gradient of the mean value of the refractive index are much larger than the laser beam size, and in Eq. (1) we take  $dn(x, z')/dz' \approx dn(x, z_c)/dz_c$ . The beam refraction is analyzed for the case of an even underlying surface assuming homogeneity of the refractive index on a sphere so that  $n(x, z_c) = n(z(x, z_c))$ , where  $z$  is the height. For horizontal paths considered here, when a source and a receiver are located at the same height  $h_s$ ,  $z(x, z_c) = [(R_E + h_s)^2 - x(L - x) + z_c^2 + z_c \sqrt{4(R_E + h_s)^2 - L^2}]^{1/2} - R_E$ , where  $R_E$  is the Earth's radius,  $L$  is the length. As a result, Eq. (1) takes the form

$$\frac{d^2 z_c}{dx^2} = m \frac{dn(z(x, z_c))}{dz}, \tag{2}$$

where  $m = dz(x, z_c)/dz_c$ . Taking into account the conditions  $R_E \gg h_s$  and  $R_E \gg L$  in Eq. (2), let us assume that  $z(x, z_c) = h_s - x(L - x)/(2R_E) + z_c$  and  $m = 1$ . We find such values of the angle  $\alpha$ , at which the beam hits to the given point of reception, i.e.,  $z_c(L) = 0$ .

### 3. VERTICAL GRADIENT OF THE REFRACTIVE INDEX

The refractive index of light for dry air under standard atmospheric conditions is determined by the expression<sup>4</sup>

$$n(z) = 1 + \nu\rho(z), \tag{3}$$

where  $\nu = 10^{-6} \cdot 222(1 + 0.0075/\lambda^2) \approx 2.22 \cdot 10^{-4} \text{ m}^3/\text{kg}$ ,  $\rho$  is the air density,  $\text{kg}/\text{m}^3$ . From the basic equation of atmospheric statics:  $dP/dz = -\rho g$ , where  $P$  is the pressure,  $g$  is the acceleration of gravity, and from the equation of the dry air state:  $P = R_c \rho T$ , where  $T$  is the absolute temperature,  $R_c = 287 \text{ m}^2/(\text{s}^2 \cdot \text{grad})$  is the gas constant, the expression can be derived for the altitude air density profile in the form

$$\rho(z) = \rho_0 \frac{T_0}{T(z)} \exp \left\{ -\gamma_A \int_{z_0}^z \frac{dz'}{T(z')} \right\}, \tag{4}$$

where  $\rho_0$  and  $T_0$  are the density and the absolute temperature at the height  $z_0$ ,  $\gamma_A = g/R_c = 3.42 \cdot 10^{-2} \text{ deg}/\text{m}$  is the temperature gradient in the homogeneous atmosphere ( $\rho = \text{const}$ ,  $d\rho/dz = 0$ ). Then for the vertical gradient of air density  $d\rho(z)/dz$  we obtain

$$\frac{d\rho(z)}{dz} = \frac{\rho_0 T_0}{T^2(z)} [\gamma(z) - \gamma_A] \exp \left\{ -\gamma_A \int_{z_0}^z \frac{dz'}{T(z')} \right\}, \tag{5}$$

where  $\gamma(z) = -\frac{dT(z)}{dz}$  is the temperature gradient represented as<sup>7</sup>

$$\gamma(z) = \gamma_a - \frac{d\theta(z)}{dz}. \tag{6}$$

In Eq.(6),  $\gamma_a = g/c_p = 0.98 \cdot 10^{-2} \text{ grad}/\text{m}$  is the adiabatic temperature gradient,  $c_p = 10^3 \text{ J}/(\text{kg} \cdot \text{deg})$  is the specific heat,  $\theta(z)$  is the potential temperature.

For the surface atmospheric layer (up to 50 m height) in Eq. (5) we can assume  $T(z) \approx T_0$  and

$$\exp \left\{ -\gamma_A \int_{z_0}^z \frac{dz'}{T(z')} \right\} \approx 1. \text{ Then from Eqs. (3), (5), and}$$

(6) for the vertical gradient of the refractive index in Eq. (2) we have

$$\frac{dn(z)}{dz} = \nu \frac{\rho_0}{T_0} \left[ \gamma_a - \gamma_A - \frac{d\theta(z)}{dz} \right]. \tag{7}$$

According to the thermodynamic theory of the surface layer,<sup>8-10</sup> the following equation can be written for the potential temperature  $\theta$ :

$$\frac{d\theta(z)}{dz} = -\frac{1}{\kappa U_*} \cdot \frac{H}{c_p \rho_0 z} \Phi_\theta(\zeta), \tag{8}$$

where  $\kappa \approx 0.4$  is the Karman constant;  $U_* = \sqrt{-\langle w' u' \rangle}$  is the friction rate (angular brackets denote the statistical averaging);  $w'$  and  $u'$  are the fluctuations of the vertical and longitudinal components of wind velocity, respectively;  $H = c_p \rho_0 \langle w' \theta' \rangle$  is the turbulent thermal flux;  $\theta'$  denotes the temperature fluctuations;  $\Phi_\theta(\zeta)$  is the universal dimensionless temperature function of the dimensionless argument  $\zeta = z/L_h$ ;  $L_h = -U_*^3 / \left( \kappa \frac{g}{T_0} \cdot \frac{H}{c_p \rho_0} \right)$  is the Monin-Obukhov scale. In its turn, the friction rate in Eq. (8) can also be expressed through the universal function  $\Phi_U(\zeta)$  for the wind velocity

$$\frac{dU(z)}{dz} = \frac{U_*}{\kappa z} \Phi_U(\zeta). \tag{9}$$

Based on the known experimental data,<sup>8-11</sup> as models of the universal functions  $\Phi_U(\zeta)$  and  $\Phi_\theta(\zeta)$  we will further use the following functions:

$$\Phi_U(\zeta) = \begin{cases} 1 + 5\zeta, & \zeta \geq 0, \\ (1 - 15\zeta)^{-1/3}, & \zeta < 0 \end{cases} \tag{10}$$

and

$$\Phi_\theta(\zeta) = \begin{cases} 0.7 + 7.75\zeta, & 0.2 \leq \zeta, \\ 0.95 + 5.24\zeta + 6.3\zeta^2, & 0 \leq \zeta < 0.2, \\ 0.95 + 5.24\zeta + 16.36\zeta^2, & -0.1 \leq \zeta < 0, \\ 0.274(-\zeta)^{-1/3}, & \zeta < -0.1. \end{cases} \tag{11}$$

From the measurements of the wind velocity and temperature at different heights of the surface layer, using Eqs. (8)–(11) we can calculate the friction rate  $U_*$  and the turbulent heat flux  $H$  (the gradient method). According to the known experimental data,<sup>8-11</sup> the value of  $H$  varies from  $-40$  to  $+400 \text{ W}/\text{m}^2$ . The friction rate  $U_*$  depends on the geostrophic wind velocity  $G$ , the roughness parameter  $z_0$ , the Coriolis parameter  $f$ , and the turbulent heat flux  $H$ . In Ref. 10 it is shown that the ratio  $U_*/G$  can vary from 0.01 to 0.1.

The sign and the value of the potential temperature gradient determine the type of temperature stratification occurring in the atmospheric boundary layer. At  $d\theta(z)/dz < 0$  the unstable temperature stratification takes place, at  $d\theta(z)/dz = 0$  the neutral temperature stratification is observed, and at  $d\theta(z)/dz > 0$  the stable temperature stratification occurs.

Consequently, at the neutral temperature stratification ( $d\theta/dz = 0$ ) the vertical gradient of the refractive index in the surface layer, in general, does not depend on the potential temperature gradient and the height above the underlying surface  $z$ , and it is determined by the difference of the adiabatic temperature gradient  $\gamma_a$  and the temperature gradient in the homogeneous atmosphere  $\gamma_A$

$$\frac{dn(z)}{dz} = \nu \frac{\rho_0}{T_0} (\gamma_a - \gamma_A). \tag{12}$$

When analyzing Eqs. (8) and (11) we deduce that at rather large negative values of heat flux  $H$  (stable stratification) when  $\zeta \geq 1$ , the gradient  $d\theta(z)/dz$  is independent of the height  $z$ , and for the gradient of the refractive index we have the expression similar to Eq. (12):

$$\frac{dn(z)}{dz} = v \frac{\rho_0}{T_0} (\gamma_a - \gamma_A - \gamma_B), \quad (13)$$

where

$$\gamma_B = \frac{7.75}{\kappa} \frac{g}{T_0} \frac{1}{U_*^4} \frac{H^2}{(c_p \rho_0)^2}. \quad (14)$$

In the case of unstable stratification ( $H > 0$ ), if  $\zeta < -0.1$ , it follows from Eqs. (8) and (11) that the gradient of potential temperature is determined by the expression

$$\frac{d\theta(z)}{dz} = - \frac{0.274}{\kappa^{7/3}} \left(\frac{T_0}{g}\right)^{1/3} \cdot \frac{H^{2/3}}{(c_p \rho_0)^{2/3}} \cdot \frac{1}{z^{4/3}} \quad (15)$$

and is independent of the friction rate  $U_*$ . In this case, with change of the height  $z$  above the underlying surface (the value  $d\theta/dz$  given by Eq. (15)) the refractive index gradient (7) may be both negative and positive due to negative value of  $d\theta(z)/dz$ . On condition that in Eq. (15)  $T_0 = 288$  deg,  $\rho_0 = 1.225$  kg/m<sup>3</sup>, for the gradient of potential temperature at  $m = 40$  W/m<sup>2</sup> we obtain  $d\theta/dz = -0.29$  deg/m at 2 m height and  $d\theta/dz = -0.034$  deg/m at 10 m height. At  $m = 400$  W/m<sup>2</sup> at the same heights the gradient  $d\theta/dz$  takes the following values:  $d\theta/dz = -1.34$  deg/m and  $d\theta/dz = -0.158$  deg/m.

It follows from Eqs. (7), (12)–(15) that the main atmospheric parameter, which characterizes the dynamics of vertical gradient of the refractive index and, consequently, the angle of regular refraction in the surface layer, is the turbulent heat flux  $H$ . The friction rate  $U_*$  may have the marked effect on the parameter  $\alpha$  only at the stable stratification. According to the experimental data,<sup>10</sup> at stable stratification the ratio  $U_*/G$  is about 0.02. Thus, for typical values of the geostrophic wind velocity  $G = 10$  m/s the value of  $U_*$  is 0.2 m/s. It is just the value of the friction rate we used for the calculations given here. The parameters  $T_0 = 288$  deg and  $\rho_0 = 1.225$  kg/m<sup>3</sup> were given according to the standard atmospheric model (All-Union State Standard 4401–64).<sup>1</sup>

#### 4. RESULTS OF REFRACTION CALCULATION

##### 4.1. Neutral Stratification

Assuming in Eq. (7) that  $d\theta/dz = 0$  and having substituted this expression into Eq. (2), after integration we obtain the following expression:

$$z_c(L) = - \frac{1}{2} v \frac{\rho_0}{T_0} (\gamma_A - \gamma_a) L^2 + \alpha L. \quad (16)$$

The refraction angle can be found from Eq. (16) as

$$\alpha = \frac{1}{2} v \frac{\rho_0}{T_0} (\gamma_A - \gamma_a) L. \quad (17)$$

It follows from Eq. (17) that at neutral temperature stratification the angle  $\alpha$  is positive, independent of height (within the surface layer), and linearly increasing with path length  $L$ .

##### 4.2. Stable Stratification

It follows from Eqs. (2) and (3) that in the limiting case of high stability of thermal stratification the refraction angle can be estimated from the asymptotic equation

$$\alpha = \frac{1}{2} v \frac{\rho_0}{T_0} (\gamma_A - \gamma_a + \gamma_B) L. \quad (18)$$

Under such conditions, it is, as for the neutral stratification, positive, height independent, and linearly increasing with  $L$ .

##### 4.3. Unstable Stratification

In the case of highly unstable temperature stratification, when calculating the refraction angle by Eq. (2), approximated equation (15) for the gradient of potential temperature can be used. Consequently, at highly unstable stratification the refraction angle  $\alpha$  is dependent on the height  $z$  and may be both positive and negative.

In the general case, Eq. (2) with the right-hand side determined by Eqs. (7), (8), and (11) was calculated numerically using the Runge-Kutta method. Using the iteration procedure the angle  $\alpha = dz_c(0)/dx$  meeting the condition  $z_c(L) = 0$  was found.

Figure 1 shows the results of calculations of the refraction angle  $\alpha$  (in angular minutes) as a function of the turbulent heat flux  $H$  for the path of length  $L = 10$  km at  $h_s = 10$  m.

From Fig. 1 it follows that at the stable stratification ( $H < 0$ ) when  $H = -20$  W/m<sup>2</sup>, the angle  $\alpha$  on this path may be as great as  $\sim 3'$ . At the unstable stratification ( $H > 0$ ), Eq. (2) with  $z_c(L) = 0$  has a solution at the two different angles of refraction  $\alpha_1$  and  $\alpha_2$  ( $\alpha_1$  is for the curve 1 and  $\alpha_2$  is for the curve 2 in Fig. 1). Analysis of Eq. (2) at arbitrary values of  $z_c(L)$  has shown that at  $\alpha_2 < \alpha < \alpha_1$  the beam coordinate  $z_c(L) < 0$ , otherwise ( $\alpha_2 > \alpha > \alpha_1$ )  $z_c(L) > 0$ . With increasing flux  $H$ , the difference in the values of  $\alpha_1$  and  $\alpha_2$  decreases and then fully vanishes at some  $H = H_{cr}$ . In this case  $H_{cr} \approx 330$  W/m<sup>2</sup>. For the flux  $H > H_{cr}$  Eq. (2) has no solution under the condition  $z_c(L) = 0$ . Thus,  $H_{cr}$  is the critical value of the turbulent heat flux for a given path, starting with which further increase of the flux  $H$  keeps the laser beam from entering the receiver  $z_c(L) = 0$  (the beam height in the observation plane will always exceed  $h_s$ ).

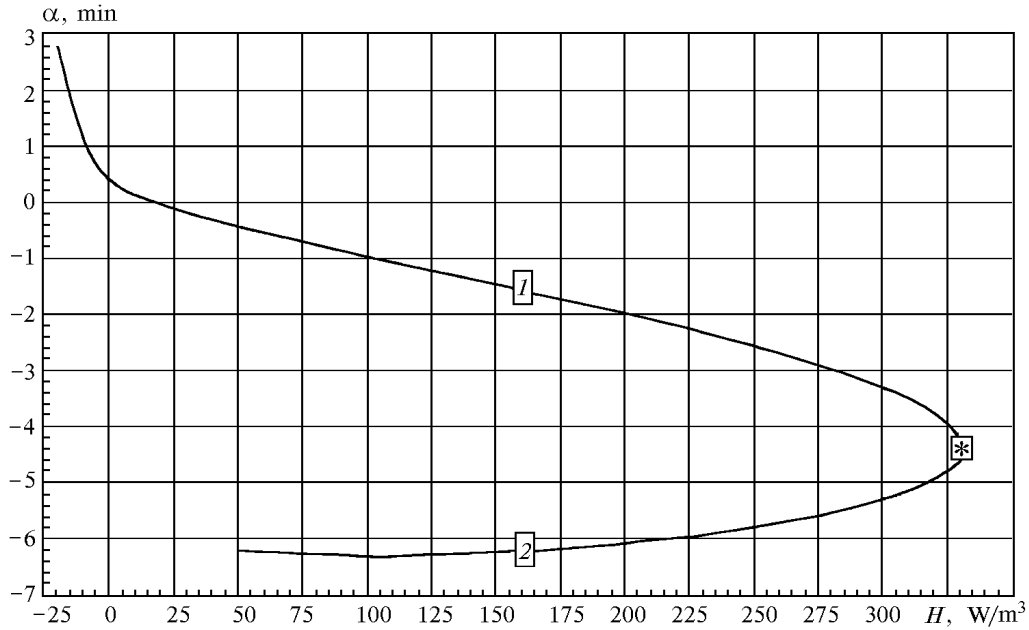


FIG. 1. The refraction angle vs. the turbulent heat flux at  $h_s = 10$  m and  $L = 10$  km.

The presence of the two solutions  $\alpha_1$  and  $\alpha_2$  of Eq. (2) at  $0 < H < H_{cr}$  is due to the focusing (vertically) effect of the medium on the optical beam. However, in practice the effect of vertical beam focusing is evidently hard to notice against a background of turbulent blooming of the beam in the receiving plane.

Figure 2 shows the change of the beam height along the propagation path at different values of the turbulent heat flux  $H$ . The dashed curve is for variation of the height  $z$  without considering the refraction ( $z_c(x) = 0$  at any  $x$ ). Curves 2 and 2' are calculated at the same value of  $H = 200$  W/m<sup>2</sup>. It is evident that in the first case the laser beam in the middle of the path drops down to the height  $z \approx 6.5$  m, in the second case the beam drops down to  $z \approx 2$  m.

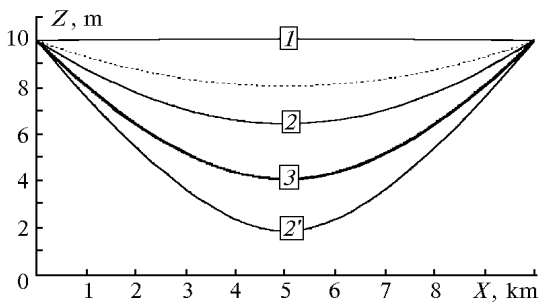


FIG. 2. Variation of the beam height along the propagation path at  $H = -20$  W/m<sup>2</sup> (1),  $H = 200$  W/m<sup>2</sup> (2 and 2'), and  $H = H_{cr} = 330$  W/m<sup>2</sup> (3).

Figure 3 shows  $L_m$  calculated as a function of the height  $h_s$  at  $H = 40$  W/m<sup>2</sup> (curve 1) and  $H = 400$  W/m<sup>2</sup> (curve 2). The pathlength  $L = L_m$  corresponds to the maximum distance at  $H = H_{cr}$ , at

which the stable optical communication between the source and the receiver at the surface horizontal path is still possible.

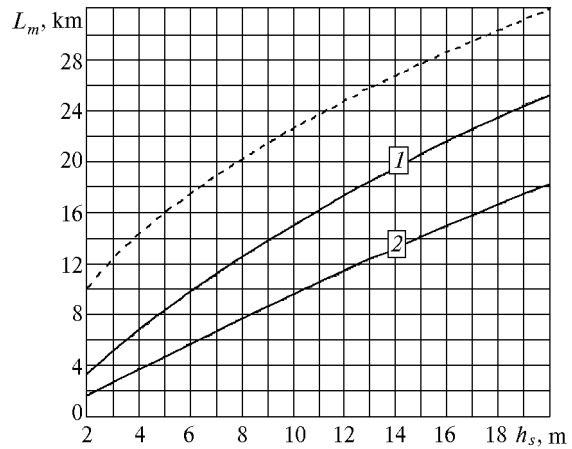


FIG. 3. The maximum pathlength  $L_m$  vs. the height  $h_s$  at  $H = 40$  W/m<sup>2</sup> (1) and  $H = 400$  W/m<sup>2</sup> (2).

According to Fig. 3, at the very unstable atmospheric stratification ( $H = 400$  W/m<sup>2</sup>), the maximum distance, at which the communication between the source and the receiver is still possible, is  $L_m \approx 1.7$  km for the source and the receiver being at 2 m height and  $L_m \approx 18$  km for the height of 20 m. It is evident that in absence of refraction ( $dn/dz = 0$ ),  $L_m \approx L_g$  where  $L_g = \sqrt{8R_E h_s}$  is the distance in a straight line connecting the points of the source and the receiver when at perigee this line is tangent to the Earth's surface because of the spherical shape of the Earth's surface.

In Fig. 3 the dependence of  $L_g$  on  $h_s$  is shown by the dashed curve. It is clear that at unstable

stratification,  $L_m$  may be several times less than  $L_g$ . At neutral and stable stratification the beam trajectory  $z(x)$  passes higher than the curve  $h_s - x(L-x) / (2R_E)$ . Therefore, in this case ( $H \leq 0$ ) optical communication is possible at distances larger than  $L_g$ .

Some examples of estimates of minimum possible shifts of the beam power centroid up from the receiver  $\Delta h_m = \min\{z_c(L)\}$  at different  $H > H_{cr}$  are presented in the Table I for the path with length  $L = 5$  km and height  $h_s = 3$  m. The value of  $H_{cr}$  for such a path is  $H_{cr} = 44 \text{ W/m}^2$ . Also given here are the values of temperature gradient  $\gamma = -dT/dz$  at the height of 3 m and estimates of the effective beam radius  $a_{ef}$  (Ref. 6) at the path end with the initial radius of 7 cm and radiation wavelength  $\lambda = 1.06 \text{ }\mu\text{m}$ .

TABLE I.

| $H, \text{ W/m}^2$       | 50    | 100   | 200   | 300   | 400   |
|--------------------------|-------|-------|-------|-------|-------|
| $\gamma, \text{ grad/m}$ | 0.206 | 0.321 | 0.503 | 0.655 | 0.792 |
| $\Delta h_m, \text{ m}$  | 0.23  | 1.52  | 3.26  | 4.55  | 5.59  |
| $a_{ef}, \text{ m}$      | 0.58  | 1.1   | 2.0   | 2.7   | 3.3   |

It is seen from the Table that the values of  $\Delta h_m$  are comparable at  $H > H_{cr}$ , and they increase the effective beam radius in the receiving plane, thus necessarily resulting in violation of communication between the source and the receiver being at the same height.

The results presented above may be useful when choosing the geometry of the optical communication (path length and height) depending on the state of the atmospheric surface layer.

REFERENCES

1. A.V. Alekseev, M.V. Kabanov, and I.F. Kushtin, *Optical Refraction in the Earth's Atmosphere (Horizontal Paths)* (Nauka, Novosibirsk, 1982), 159 pp.
2. V.V. Vinogradov, *Effect of the Atmosphere on the Geodesic Measurements* (Nedra, Moscow, 1992), 253 pp.
3. A.L. Ostrovskii, B.M. Dzhuman, and F.D. Zablotskii, *Consideration of Atmospheric Effect on the Astrogeodezic Measurements* (Nedra, Moscow, 1990).
4. A.S. Gurvich and S.V. Sokolovskii, Tr. S.I. Vavilov State Optical Institute **71**, No. 205, 18–49 (1989).
5. G.S. Golitsin, Izv. Akad. Nauk SSSR, Fiz. Atmos. Okeana **18**, No. 5, 1282–1288 (1982).
6. A.S. Gurvich, A.I. Kon, V.L. Mironov, and S.S. Khmelevtsov, *Laser Radiation in the Turbulent Atmosphere* (Nauka, Moscow, 1976), 227 pp.
7. L.T. Matveev, *Course of General Meteorology* (Gidrometeoizdat, Leningrad, 1976), 639 pp.
8. A.C. Monin and A.M. Yaglom, *Statistical Hydromechanics*, (Nauka, Moscow, 1967), Vol. 2, 720 pp.
9. I.L. Lumley and H.A. Panofsky, *The Structure of Atmospheric Turbulence* (Interscience, New York, 1964).
10. S.S. Zilitinkevich, *Dynamics of the Atmospheric Boundary Layer* (Gidrometeoizdat, Leningrad, 1970), 290 pp.
11. U. Högström, Boundary-Layer Meteorology **42**, 55–78 (1988).